Published in final edited form as:
J Immunol. 2014 February 15; 192(4): 1862–1869. doi:10.4049/jimmunol.1302147.

Heterotropic modulation of selectin affinity by allosteric antibodies affects leukocyte rolling

Sebastian B Riese[*], **Christian Kuehne**[*], **Thomas F Tedder**[†], **Rupert Hallmann**[‡], **Erhard Hohenester**[¶], and **Konrad Buscher**[‡,‖,#]

[*]Institute of Laboratory Medicine, Clinical Chemistry and Pathobiochemistry, Charité – Universitätsmedizin Berlin, Berlin, Germany

[†]Department of Immunology, Duke University Medical Center, Durham, North Carolina, USA

[‡]Institute of Physiological Chemistry and Pathobiochemistry, University of Münster, Münster, Germany

[¶]Department of Life Sciences, Imperial College London, London, United Kingdom

[‖]Department of Anesthesiology, Intensive Care, and Pain Medicine, University of Münster, Münster, Germany

Abstract

Selectins are a family of adhesion receptors designed for efficient leukocyte tethering to the endothelium under shear. As a key property to resist premature bond disruption, selectin adhesiveness is enhanced by tensile forces that promote the conversion of a bent into an extended conformation of the N-terminal lectin and EGF-like domains. Conformation-specific antibodies have been invaluable in deciphering the activation mechanism of integrins, but similar reagents are not available for selectins. Here we show that the anti-human L-selectin monoclonal antibodies DREG-55 and LAM1.5 but not DREG-56, -200 or LAM1.1 heterotropically modulate adhesion presumably by stabilizing the extended receptor conformation. Force-free affinity assays, flow chamber and microkinetic studies reveal a ligand-specific modulation of L-selectin affinity by DREG-55 mAb, resulting in a dramatic decrease of rolling velocity under flow. Furthermore, secondary tethering of polymorphonuclear cells was blocked by DREG-200 but significantly boosted by DREG-55 mAb. The results emphasize the need for a new classification for selectin antibodies and introduce the new concept of heterotropic modulation of receptor function.

Keywords

selectin; adhesion; catch bonds; leukocyte; rolling; dreg-55

INTRODUCTION

Leukocyte tethering to and rolling on the vascular endothelium represents the first step of the adhesion cascade and is mediated by the selectin receptor family in most physiological and pathological conditions (1).

[#]corresponding author: Konrad Buscher, M.D., Institute of Physiological Chemistry and Pathobiochemistry, University of Münster, Münster, Germany kbuscher@uni-muenster.de Tel.: 0049 251 83 55583 Fax.: 0049 251 83 55596 .
Author contributions: Experiments were performed by S.R., K.B., and C.K.. T.T. provided LAM antibodies. E.H. analyzed the structural implications. K.B. designed the study and analyzed data. K.B and R.H. wrote the manuscript.

Europe PMC Funders Author Manuscripts

E- (endothelium), P- (platelet) and L- (leukocyte) selectin are calcium-dependent type I adhesion receptors. They consist of an N-terminal lectin domain followed by an EGF-like domain, a varying number of short consensus repeats, a single transmembrane domain and a short intracellular tail (2). A common minimal ligand determinant was identified as the tetrasaccharide sialyl Lewis x (sLe^x) with terminal α2,3-linked sialic acid and α1,3-linked fucose units that decorate a variety of O-glycans, e.g. the leukocyte-expressed P-selectin glycoprotein ligand 1 (PSGL-1). In most inflammatory conditions, E- and P-selectin are major counter-receptors for PSGL-1 but also trans-interactions with L-selectin (CD62L) on passing leukocytes were found to be relevant for mediating secondary capture (3, 4). In lymphoid tissue, particularly in high endothelial venules (HEV), the predominant ligand entity for L-selectin-mediated rolling is peripheral lymph node addressin (PNAd), a molecular complex of different sialomucins (5). Importantly, only sLe^x with sulfated N-acetylglucosamine (6-sulfo-sLe^x) on PNAd shows L-selectin binding activity (5). The great variety of different ligands, selectin expression patterns, and relevant post-translational modifications reflects the precise tissue- and cell-type specific manner of leukocyte recruitment.

By nature, the bonds that bind selectin to endothelial or leukocyte expressed ligands are subjected to high tensile forces imposed by hydrodynamic flow. Cell flattening (6), microvillus receptor presentation (7, 8), the formation of upstream membrane tethers and downstream slings (9) describe cell adaptions to rolling under high shear. Importantly, also intrinsic receptor binding properties effectively modulate bond stability. A threshold of shear force is required for L-selectin-mediated binding which was the first indication of the striking role of blood flow on selectin mechanics (10). Leukocyte rolling on immobilized ligands requires selectins to engage in fast but transient ligand interactions with high association (k_{on}) and dissociation rates (k_{off}) (11). Surprisingly, it was demonstrated that tensile forces enhance selectin-mediated adhesion and stabilize cell rolling by decreasing k_{off} in low shear conditions (12, 13), promoting the formation of so-called ‘catch bonds’.

The first study on altered L-selectin receptor function detected affinity changes upon leukocyte activation, however, the precise mechanism remained unresolved (14). Domain swapping experiments suggested a role for the EGF-like domain in ligand binding (15, 16) and crystal structure analysis subsequently revealed a flexible hinge between the N-terminal lectin and EGF-like domain of selectins (17, 18). While sLe^x is bound by a bent conformation of P-selectin, co-crystallization with PSGL-1 glycopeptide revealed an extended conformation (17). The transition from the bent to the extended state involves several subdomain movements in the lectin domain (19). One major component of this allosteric pathway is the 83-89 loop that relocates in close vicinity to the ligand binding interface. Thereby new non-covalent interactions are formed, including Glu-88 ligation to the calcium ion and the PSGL-1 fucose unit, and Arg-85 binding to a sulfated tyrosine of the PSGL-1 polypeptide. A second sulfate tyrosine is bound by His-114 in P-selectin. The corresponding residue in L-selectin is alanine, a substitution that partially explains the lower affinity of L-selectin for PSGL-1 (20). To date, L-selectin crystal data are available only for the unbound state (PDB 3CFW), but the high phylogenetic conservation and molecular dynamic simulations suggest fundamentally similar ligand binding modes for all selectins (21).

Tensile forces acting on a selectin-ligand complex favor the extended conformation, aligning the long axis of receptor with the direction of the force applied (21, 22). It is believed that this property gives rise to ‘catch bonds’, however, there is no clear consensus about the underlying mechanism. In the ‘allosteric model’, pivoting about the EGF-lectin interdomain hinge causes a restructuring of the distal ligand binding interface to a high affinity conformation (19, 22). In contrast, the ‘sliding-rebinding’ model is based on

alignment of the lectin domain with the acting force, thereby enabling repetitive contacts to several carbohydrate epitopes on the same ligand (21, 23).

In all studies on selectin mechanochemistry, only genetically modified receptors have been studied (21, 22, 24). This is due to the fact that, in contrast to e.g. integrins, no reagents are known that modulate specific conformational states of selectins. We discovered that the anti-L-selectin monoclonal antibodies (mAb) DREG-55 and LAM1.5 dramatically reduce L-selectin-mediated lymphocyte rolling velocity under shear, consistent with the selective binding to a high-affinity conformation of L-selectin. This data introduce the new concept of heterotropic modulation of selectin affinity and demonstrate how such anti-selectin mAbs can provide further insights on the structure-function relationship. Moreover, our data highlight the need for a new classification of anti-selectin mAbs according to their distinct stimulatory or inhibitory activities.

MATERIALS AND METHODS

Reagents and antibodies

Hanks-balanced salt solution (HBSS) containing Ca^{2+} and Mg^{2+} was obtained from Invitrogen. DREG-55 and -200 mAb hybridomas were a kind gift from E. Butcher (Stanford University). DREG-56 (sc-18851) was purchased from Santa Cruz Biotechnology and the secondary antibody goat anti-human IgG (F_c specific)-FITC (F9512) from Sigma Aldrich. Mouse anti-human L-selectin LAM1.1 and LAM1.5 monoclonal antibodies were collected from ascites fluid (16). Purified human L-selectin-, PSGL-1- and E-selectin-F_c chimeras were obtained from R&D Systems. PNAd extracts from human tonsils were kindly provided by S. Rosen (University of California, San Francisco). Streptavidin was from Calbiochem and biotinylated sLe^x-polyacrylamide(PAA) from Lecinity (Moscow, Russia). DREG-55 F_{ab} fragments were generated with an IgG_1 F_{ab} purification kit according to the manufactor's instructions (Thermo Scientific). SDS-PAGE under reducing and non-reducing conditions confirmed the generation of monovalent F_{ab} and the exclusion of F_c.

Cell isolation and culture

The Jurkat cell line clone E6-1 (ATCC) was cultured in RPMI 1640 medium supplemented with 10% FCS and penicillin/streptomycin at 37°C and 5% CO_2. EDTA-anticoagulated blood was obtained from healthy volunteers and separated by a Ficoll 1.077 and 1.119 g/ml gradient. The isolation yielded > 90% viable human primary blood lymphocytes (PBL) and polymorphonuclear leukocytes (PMN) as verified by flow cytometry. Isolated cells were kept on ice for a maximum of 4 h.

L-selectin coated microspheres

Carboxylated polystyrol microspheres (beads, 6 μm diameter) were coupled to protein G using a carbodiimide coupling kit (Polysciences). Human L-selectin-F_c (complete extracellular domain of L-selectin) was incubated with the beads for 1 h at room temperature, subsequently blocked by 2 mg/ml bovine serum albumin in phosphate-buffered saline (PBS) and successful coating was verified by flow cytometry. Protein G coupled beads without addition of L-selectin-F_c did not show any interaction in PSGL-1 coated flow chambers under shear.

Flow cytometry based affinity assay

3×10^6 Jurkat cells were washed in calcium-free PBS and resuspended in HBSS buffer. 10 μg/ml DREG-55 mAb, −200 mAb or PBS (untreated) and 10 μg/ml PSGL-1-F_c or E-selectin-F_c were added and incubated for 10 min at room temperature. After washing, cells were resuspended in ice-cold PBS/1% FCS buffer followed by a 30 min incubation with

1:1000 anti-human IgG-FITC on ice. Flow cytometry was performed and the mean fluorescence intensity (MFI) was calculated relative to the sample with DREG-200 antibody (negative control).

Laminar flow assays

Ibidi μ-slides $VI^{0.1}$ (0.1 mm high) were coated for 2 h at room temperature with 30 μg/ml PSGL-1-F_c or 5 μg/ml E-selectin-F_c, unless otherwise stated, followed by 1h blocking with 2 mg/ml BSA in PBS. Alternatively, PNAd was applied overnight at 4°C. For flow chambers on sLe^x, 10 μg/ml streptavidin coating overnight at 4°C was followed by 20 μg/ml biotinylated sLe^x-PAA coating for 2 h at room temperature. 0.3×10^6 cells/ml in HBSS were preincubated for 5 min with the indicated antibody at room temperature. For representative video recordings, the antibody was directly added to the distal cell suspension reservoir of the running flow chamber system. Digital videos were recorded with an inverted phase contrast microscope (Axiovert M200, Zeiss) equipped with a CCD-camera (ORCA, Hamamatsu) at 37°C and 10× magnification. Cells were introduced at a high flow rate (> 20 dyn/cm^2) for 1 min, and the flow rate was subsequently adjusted to the desired shear stress level. After an equilibration of 2 min, at least 3 different field of views (FOV) were recorded. Rolling velocities were determined by offline analysis using Fiji (25). For detachment assays, cells were allowed to settle and the flow rate was increased step-wise to 1, 1.5, 3, 6 and 10 dyn/cm^2. After one minute of equilibration, a snapshot of 3 different FOVs were taken and the number of interacting cells were counted and expressed relative to 1 dyn/cm^2. PMN string formation was analyzed using 20 μg/ml E-selectin coated chambers after 3 min equilibration of flow and 6 adjacent FOVs (~ 1300 × 1000 μm) were recorded. More than three cells aligned in direction of the flow with at most 5 cell diameters distance between two cells were considered a string.

Microkinetic velocity measurement

For motion analysis in high-temporal resolution, digital videos were aquired at 20× or 40× magnification with 100 fps (Neo 5.5 sCMOS camera, Andor) at room temperature. The recorded rolling motion was then subjected to an automated frame-by-frame analysis using a snake-model based algorithm in Matlab (MathWorks Inc.). X-coordinates were translated into step distances and velocities by customized Excel macros. At 0.96 dyn/cm^2 a velocity threshold of 28 μm/s was found suitable for discriminating between load-bearing (deceleration) and breaking (acceleration) bonds in untreated and DREG-55 antibody treated (10 μg/ml) samples. Measurements were repeated twice in triplicates with 13 - 16 analyzed cells per group, totaling 68 – 116 tether events. The logarithmic expression of tethered cells allowed the determination of $-k_{off}$ from the slope of the linear regression. Importantly, under the experimental conditions used this value is only an apparent k_{off} due to multibond tethers, however, it can be used for comparison of dissociation kinetics in the same cellular system.

Statistics

The significance of results was determined using the Student's t test. P value * < 0.05, ** < 0.01, *** < 0.001, ns = not significant.

RESULTS

DREG-55 and LAM1.5 antibodies induce L-selectin-mediated slow lymphocyte rolling

L-selectin dependent rolling was investigated in a parallel plate flow chamber on the immobilized ligand PSGL-1-F_c. Untreated primary blood lymphocytes (PBL) showed fast and stable rolling at 2 dyn/cm^2 (Figure 1A). Anti-human L-selectin mAb DREG-200

blocked any interactions proving the specificity of rolling (not shown). DREG-55 mAb but not isotype anti-human IgG_1 preincubation at saturating concentrations triggered a massive decrease in mean rolling velocity from 113 to 13 μm/s. Fast rolling was directly converted into slow homogenous rolling within a subsecond period and hardly any detachment of cells was observed (Video 1). Minimal and maximal velocities measured were 48 and 136 μm/s for untreated and 9 and 28 μm/s for treated PBL, respectively, showing a more uniform slow rolling phenotype. To investigate whether this effect includes a cellular response, the assay was repeated using L-selectin coated microspheres yielding comparable results (Figure 1A).

A similar phenotype was observed using human primary polymorphonuclear cells (PMN, not shown) and the human T lymphocyte cell line Jurkat (Figure 1B). Importantly, monovalent DREG-55 mAb F_{ab} antibody fragment was sufficient to reduce rolling velocity, excluding F_c receptor participation and dimerization effects. Additional DREG-200 mAb, EDTA or KPL-1 mAb (blocking anti-human PSGL-1 mAb) treatment blocked the slow rolling interaction and induced detachment showing the L-selectin dependent nature of this phenomenon (Figure 1B). DREG-55 antibody titration revealed a concentration dependent effect, with 10 μg/ml yielding the lowest velocity (Figure 1C). Further increase up to 100 μg/ml did not significantly alter rolling further (not shown).

To investigate DREG-55 antibody implications on shear resistance, Jurkat cells were allowed to settle onto a PSGL-1-F_c coated flow chamber in the presence or absence of DREG-55, followed by step-wise increase of shear and the number of rolling cells at each shear level was measured. The proportion of slow rolling Jurkat cells in the presence of DREG-55 mAb was reduced with increasing shear compared to untreated cells (Figure 1D). In a range from 1 to 6 dyn/cm^2 no significant change in the rolling flux of untreated cells was detected, whereas DREG-55 antibody treatment promoted detachment already at 1.5 dyn/cm^2 with complete abolishment of rolling at 6 dyn/cm. Similarly, the capture rate was significantly decreased by DREG-55 mAb (not shown)

It was reported previously that monoclonal anti-human L-selectin antibodies of the LAM-family showed stimulatory L-selectin binding activity in a soluble binding assay using polyphosphomonoester polysaccharide (PPME) or fucoidan (16, 26). Indeed, LAM1.5 antibody significantly reduced the rolling velocity of Jurkat cells on PSGL-1 by 36% while another member of this family, LAM1.1, exerted full inhibitory function (Figure 1E).

Bond dissociation rates are decreased by DREG-55 antibody

Since ligand density is a crucial parameter affecting rolling mechanics, we investigated the impact of increased ligand spacing. Dilution of immobilized PSGL-1-F_c revealed 6 μg/ml to be the minimal coating concentration required to support rolling at 2 dyn/cm^2. A significant increase in rolling velocity was already observed at 10 μg/ml but more accentuated at 6 μg/ml PSGL-1-F_c using untreated Jurkat cells. However, DREG-55 antibody treatment triggered similar slow rolling velocities at all densities of PSGL-1-F_c tested (Figure 2A), suggesting decreased bond dissociation.

Next, microkinetic analysis on low density ligand was performed at high temporal resolution (100 fps, suppl. video 2). Figure 2B depicts a representative velocity profile of an individual untreated Jurkat cell over 2 seconds at 0.96 dyn/cm^2. Regular cell decelerations with intermitting accelerations from 6 to 300 μm/s were observed. Notably, at the applied shear stress and frame rate, no complete cell arrest was detected. The addition of DREG-55 mAb dramatically altered the microkinetics of L-selectin dependent rolling. Enduring slow motions ranging from complete stop to 15 μm/s were interrupted by short forward movements at medium velocity (Figure 2D). Although the velocity patterns most likely represent multibond interactions in this experimental setup, a comparative k_{off} was

determined on the basis of tether durations as described in materials and methods, revealing an almost 10-fold increase (Figure 2C). Step distances were markedly reduced from 20.9 to 1.2 μm upon DREG-55 mAb treatment (not shown).

DREG-55 mAb induced slow rolling is ligand specific

Physiological L-selectin ligand epitopes vary considerably. While a crucial binding motif in PSGL-1 includes the sulfated tyrosine residues of the protein scaffold in addition to an adjacent core-2-based *O*-glycan capped with sLe^x (27), binding to HEV-expressed PNAd depends on 6-sulfo-sLe^x carbohydrates (5).

Immobilized PSGL-1-F_c, E-selectin-F_c, PNAd and sLe^x supported specific L-selectin mediated rolling of Jurkat cells (Figure 3). However, only PSGL-1-F_c and E-selectin-F_c were sufficient to allow DREG-55 induced slow rolling, whereas on PNAd and sLe^x all rolling cells detached. In contrast, DREG-200 antibody blocked rolling on all ligands (not shown). A similar selective modulation of rolling on PSGL-1-F_c and E-selectin- F_c was obtained using DREG-55 mAb F_{ab} fragments (not shown). These results indicate that specific ligand requirements for DREG-55 mAb-induced L-selectin-mediated slow rolling are met by PSGL-1 and E-selectin but not by sLe^x or PNAd.

Shear-free affinity of L-selectin is upregulated by DREG-55 antibody

To directly address the question of force-free (shear-independent) affinity modulation, a flow cytometry based assay for ligand affinity was performed. Jurkat cells were incubated with or without mouse anti-human DREG-55 or -200 antibody together with soluble human PSGL-1-F_c or E-selectin-F_c chimeric proteins and the specific binding of a secondary anti-human IgG-FITC antibody was detected. Samples with the blocking DREG-200 antibody served as negative control. As L-selectin bonds are characterized by low affinity interactions (28), the binding of soluble E-selectin-F_c or PSGL-1-F_c to untreated Jurkat cells was absent under these experimental conditions (Figure 4). DREG-200 mAb did not induce significant changes relative to untreated samples excluding possible cross-reactions of the anti-human IgG antibody to mouse DREG-Ig or of DREG antibodies to cellular F_c receptors. By contrast, coincubation of Jurkat cells with DREG-55 mAb lead to a 1.6 and 1.4 fold higher binding of soluble PSGL-1-F_c and E-selectin-F_c, respectively. This result suggests that the treatment of Jurkat cells with DREG-55 mAb exposes a higher affinity binding site on the L-selectin molecule in the absence of shear (Figure 4).

Secondary capture of PMNs is amplified by DREG-55 mAb

Intercellular interactions between free flowing and adherent neutrophils occur via transient PSGL-1-L-selectin bonds and serve as a mechanism to boost neutrophil recruitment at inflammatory sites (‘secondary capturing’) (29). Using isolated PMN under flow, the formation of cells lined up in the direction of the flow (strings) can be observed in vitro. As L-selectin shows a higher affinity to PSGL-1 in the DREG-55 mAb modified state (Figure 4), we investigated whether there is a functional relevance in secondary capture. Therefore, untreated, DREG-55 or -200 mAb F_{ab} fragment treated human PMNs were perfused into a E-selectin coated flow chamber at 1 dyn/cm^2. An average of ~ 2 strings/FOV was found in untreated conditions and addition of DREG-200 mAb F_{ab} abolished most of the secondary but not primary capture (Figure 5A, B). In contrast, DREG-55 mAb F_{ab} treatment intensified string formation and yielded longer strings (Figure 5B, C).

DREG-55 antibody targets switch regions of L-selectin

Previous random mutagenesis of human L-selectin had identified the amino acid positions 11, 56, 87, 89, 105, 107 and 111 as critical for DREG-55 mAb binding (30) (Figure 6A).

Since only the bent conformation of L-selectin has been crystallized to date, we mapped these positions onto the bent and extended conformations of P-selectin (Figure 6B). Three of the critical residues (105, 107, 111) surround the calcium binding site and are unlikely to be involved directly in DREG-55 mAb binding. Residues 55, 87 and 89 (and possibly 11) form a plausible convex epitope. Interestingly, these residues are located in the two major switch regions that allosterically couple selectin extension to increased affinity for ligand (19). DREG-200 mAb interacts with a distant region unaffected by conformational changes at L-selectin residues 45, 46 and 47 (30) and the latter is known to interact with the sulfated Tyr-7 (Tyr-48 of the propeptide) of PSGL-1, thus explaining its blocking activity (Figure 6B) (31).

DISCUSSION

Selectin-mediated tethering and rolling under shear is dependent on multiple factors, e.g. receptor binding kinetics. However, the role of different selectin conformations in bond stabilization is not yet fully understood. To this end, we analyzed the allosteric impact of different antibodies on selectin rolling with the conclusion that 1) selectin-mediated rolling can be regulated by exogenous soluble molecules without directly interfering with the binding site for the ligand PSGL-1, 2) the anti-L-selectin mAbs LAM1.5 and DREG-55 show such activity, the latter presumably by enforcing a loop reorientation in the lectin domain, and 3) a high-affinity conformation of L-selectin can be adopted in shear-free conditions supporting the allosteric model of catch bonds.

L-selectin is well known as a signaling molecule (32, 33). Hence, the increase in L-selectin mediated ligand binding could result from outside-in signaling events leading to reorganization of adhesion receptors on the leukocyte surface (34). However, several lines of evidence argue against this in DREG-55 antibody induced slow rolling: First, anti-L-selectin or anti-PSGL-1 blocking antibodies abolish lymphocyte interaction in both DREG-55 mAb-treated and untreated samples completely (Figure 1B) excluding the involvement of integrins or other adhesion molecules. Second, our own unpublished data demonstrates that energy depletion by azide and 2-deoxy-glucose in Jurkat cells does not impair the observed phenotype. Third, neither the use of F_{ab} fragments (Figure 1B) nor confocal imaging (not shown) supported a role for receptor dimerization or clustering, respectively. Finally, slow rolling was also inducible using microspheres coated with the extracellular domain of human L-selectin (Figure 1A). We therefore conclude that the observed findings are best explained by an effect of DREG-55 mAb on an intrinsic property of the L-selectin molecule and not by avidity or signaling-dependent effects.

Analysis of the DREG-55 mAb binding site and investigation of its functional impact provides some information on the underlying structural mechanisms governing the slow rolling phenotype. It is known that sLe^x binds to P-selectin in the bent state whereas the ligand PSGL-1 triggers the extended conformation, thereby enabling additional bonds to sulfated tyrosines of the PSGL-1 backbone (27, 35). Since the 83-88 loop of the L-selectin lectin domain is targeted by DREG-55 mAb (Figure 6) and this loop binds the Tyr-7 residue of PSGL-1 only in the extended conformation (17), we hypothesize that this loop movement is important for the observed increase of L-selectin affinity to PSGL-1. Flow chamber assays using different ligands support this hypothesis. DREG-55 antibody decelerated L-selectin-mediated leukocyte rolling only on PSGL-1 and E-selectin, whereas on PNAd and sLe^x it exerted blocking functions (Figure 3). This differential support of DREG-55 mAb on rolling indicates that specific structural requirements of the ligand are necessary to stabilize the bonds to the DREG-55 mAb-enforced selectin conformation, e.g. sulfated tyrosines that are available on PSGL-1 but not on sLe^x. Despite the use of F_{ab} fragments, we cannot exclude that steric hindrance is responsible for the inability of antibody-occupied L-selectin

to adhere to immobilized PNAd or sLe^x. Furthermore it should be noted that selectin bonds to sulfated tyrosines alone are not sufficient for high affinity binding but rather require additional bonds to adjacent carbohydrate units (31).

In humans, E-selectin is a L-selectin ligand of unknown physiological relevance (36, 37). Since E-selectin also supports DREG-55 antibody induced slow rolling, with a similar reduction in velocity of rolling (74%) as observed with cells rolling on PSGL-1 (Figure 3), it is tempting to spectulate on a common ligand motif, in both E-selectin and PSGL-1. However, the absence of detailed functional and structural data from E-selectin-L-selectin bonds prevents investigation of this possibility.

An important question is how the increased selectin affinity under static conditions induced by DREG-55 mAb (Figure 4) translates to lower shear resistance (Figure 1D). A similar counter-intuitive behavior was described for the A28H mutant of P-selectin (24). This mutation filled a structural cleft within the lectin domain favoring the extended state with high affinity binding to PSGL-1. Similar to our assumptions on DREG-55 mAb, a predicted allosteric change was the movement of the 83-89 loop. Yeast expressing this mutant also showed a decreased rolling velocity on immobilized PSGL-1-F_c compared to wildtype P-selectin but detached faster at higher shear forces. It was hypothesized that this behavior might result from a slower interconversion between bent and extended states in the mutant. These data are very similar to those obtained here, supporting the allosteric model of selectin mechanochemistry with a 2-state conformational equilibrium (24). We postulate that DREG-55 mAb binds specifically to the extended conformation of L-selectin and thereby increases the equilibrium constant in a concentration-dependent manner (Figure 2C), resulting in enhanced ligand binding in shear-free conditions. An analogous mechanism is well documented for activating anti-integrin antibodies (38–40).

The DREG family of antibodies was raised by Kishimoto et al. against a downregulated (DREG) adhesion molecule on PMA-activated human lymphocytes that blocked L- selectin binding in frozen section assays of lymphoid tissue (41). DREG-55, DREG-56 and DREG-200 mAbs have been widely employed as blocking antibodies ever since. The fact that DREG-55 mAb indeed blocks L-selectin binding to HEV-expressed PNAd and mAb-induced slow rolling on PSGL-1 becomes unstable with increasing shear could explain why the allosteric activity has been overlooked for many years. Although our data provide the first detailed description on activating anti-selectin mAbs under flow, evidence for other such mAbs has been reported previously, however, without recognition of their role in mechanochemistry. Shear-free affinity assays showed higher binding signals for the artifical L-selectin ligands polyphosphomonoester (PPME) and Fucoidan in the presence of LAM1-1 or LAM1-5 (16, 26). Our data indicate that LAM1.5 but not LAM1.1 mAb modulates L-selectin-mediated rolling on PSGL-1 under physiological shear (Figure 1E). Published data and our own findings on anti-human selectin mAbs targeting the lectin domain are summarized in Table I .

The investigation of the complex affinity regulation of heterodimeric integrins was greatly facilitated by the use of conformation-sensitive antibodies. Extensive work on functional residue mapping provided valuable insights on intramolecular remodeling and served as useful reagents to analyze mechanisms of action (42, 43). Non-functional, stimulatory/activation-specific and inhibitory categories classify integrin antibodies according to their molecular activity. Precise knowledge about antibody effects is of high relevance as it can shed light on the structure-function relationship of selectins and the wrong choice might adversely affect the interpretation of experimental data. In light of the results presented here, we propose a similar classification system for selectin antibodies.

Europe PMC Funders Author Manuscripts

Our data indicate that L-selectin-mediated rolling can be regulated by exogenous molecules that do not block ligand recognition. This may be explained by the 'allosteric pathway', whereby alterations at sites distant to the ligand trigger changes in the binding interface through 'transmission of allostery' (19, 24) and implies important functional consequences. We show that DREG-55 mAb renders more effective secondary tethering of PMNs (Figure 5), a mechanism highly important for inflammatory neutrophil recruitment in vivo (29). It is therefore conceivable to develop small-molecule probes that induce or inhibit specific selectin conformations as a new therapeutic approach to modulate inflammation or lymphocyte homeostasis.

Supplementary Material

Refer to Web version on PubMed Central for supplementary material.

Acknowledgments

We are grateful to Klaus Ley for general advice, Steven Rosen for providing PNAd, Yaroslav Tsytsyura for technical support with microkinetic measurements and Lydia Sorokin for critical reading of the manuscript.

This work was funded by a Interdisziplinäres Zentrum für Klinische Forschung (IZKF) grant of the University of Muenster to K.B. (SEED 04/12). E.H. is a Wellcome Trust Senior Research Fellow in Basic Biomedical Science (083942/Z/07/Z).

Glossary

EGF	Epidermal growth factor
FOV	Field of view
HEV	High endothelial venules
PPME	polyphosphomonoester
PSGL-1	P-selectin glycoprotein ligand 1
SCR	Short consensus repeats
sLe^x	Sialyl Lewis x [NeuAc-α2,3-Gal-β1,4-(Fuc-α1,3)GlcNAcβ1-R]

REFERENCES

1. Ley K, Laudanna C, Cybulsky MI, Nourshargh S. Getting to the site of inflammation: the leukocyte adhesion cascade updated. Nat. Rev. Immunol. 2007; 7:678–689. [PubMed: 17717539]
2. McEver RP. Selectins: lectins that initiate cell adhesion under flow. Curr. Opin. Cell Biol. 2002; 14:581–586. [PubMed: 12231353]
3. Bargatze RF, Kurk S, Butcher EC, Jutila MA. Neutrophils roll on adherent neutrophils bound to cytokine-induced endothelial cells via L-selectin on the rolling cells. J. Exp. Med. 1994; 180:1785–1792. [PubMed: 7525838]
4. Tu L, Murphy PG, Li X, Tedder TF. L-selectin ligands expressed by human leukocytes are HECA-452 antibody-defined carbohydrate epitopes preferentially displayed by P-selectin glycoprotein ligand-1. J. Immunol. Baltim. Md 1950. 1999; 163:5070–5078. [PubMed: 10528213]
5. Rosen SD. Ligands for L-selectin: homing, inflammation, and beyond. Annu. Rev. Immunol. 2004; 22:129–156. [PubMed: 15032576]
6. Firrell JC, Lipowsky HH. Leukocyte margination and deformation in mesenteric venules of rat. Am. J. Physiol. - Heart Circ. Physiol. 1989; 256:H1667–H1674. [PubMed: 2735435]
7. Von Andrian UH, Hasslen SR, Nelson RD, Erlandsen SL, Butcher EC. A central role for microvillous receptor presentation in leukocyte adhesion under flow. Cell. 1995; 82:989–999. [PubMed: 7553859]

8. Buscher K, Riese SB, Shakibaei M, Reich C, Dernedde J, Tauber R, Ley K. The transmembrane domains of L-selectin and CD44 regulate receptor cell surface positioning and leukocyte adhesion under flow. J. Biol. Chem. 2010; 285:13490–13497. [PubMed: 20212041]
9. Sundd P, Gutierrez E, Koltsova EK, Kuwano Y, Fukuda S, Pospieszalska MK, Groisman A, Ley K. "Slings" enable neutrophil rolling at high shear. Nature. 2012; 488:399–403. [PubMed: 22763437]
10. Finger EB, Puri KD, Alon R, Lawrence MB, von Andrian UH, Springer TA. Adhesion through L-selectin requires a threshold hydrodynamic shear. Nature. 1996; 379:266–269. [PubMed: 8538793]
11. Alon R, Chen S, Puri KD, Finger EB, Springer TA. The kinetics of L-selectin tethers and the mechanics of selectin-mediated rolling. J. Cell Biol. 1997; 138:1169–1180. [PubMed: 9281593]
12. Marshall BT, Long M, Piper JW, Yago T, McEver RP, Zhu C. Direct observation of catch bonds involving cell-adhesion molecules. Nature. 2003; 423:190–193. [PubMed: 12736689]
13. Yago T, Wu J, Wey CD, Klopocki AG, Zhu C, McEver RP. Catch bonds govern adhesion through L-selectin at threshold shear. J. Cell Biol. 2004; 166:913–923. [PubMed: 15364963]
14. Spertini O, Kansas GS, Munro JM, Griffin JD, Tedder TF. Regulation of leukocyte migration by activation of the leukocyte adhesion molecule-1 (LAM-1) selectin. Nature. 1991; 349:691–694. [PubMed: 1705015]
15. Kansas GS, Saunders KB, Ley K, Zakrzewicz A, Gibson RM, Furie BC, Furie B, Tedder TF. A role for the epidermal growth factor-like domain of P-selectin in ligand recognition and cell adhesion. J. Cell Biol. 1994; 124:609–618. [PubMed: 7508943]
16. Spertini O, Kansas GS, Reimann KA, Mackay CR, Tedder TF. Function and evolutionary conservation of distinct epitopes on the leukocyte adhesion molecule-1 (TQ-1, Leu-8) that regulate leukocyte migration. J. Immunol. 1991; 147:942–949. [PubMed: 1713609]
17. Somers WS, Tang J, Shaw GD, Camphausen RT. Insights into the molecular basis of leukocyte tethering and rolling revealed by structures of P- and E-selectin bound to SLe(X) and PSGL-1. Cell. 2000; 103:467–479. [PubMed: 11081633]
18. Graves BJ, Crowther RL, Chandran C, Rumberger JM, Li S, Huang KS, Presky DH, Familletti PC, Wolitzky BA, Burns DK. Insight into E-selectin/ligand interaction from the crystal structure and mutagenesis of the lec/EGF domains. Nature. 1994; 367:532–538. [PubMed: 7509040]
19. Springer TA. Structural basis for selectin mechanochemistry. Proc. Natl. Acad. Sci. U. S. A. 2009; 106:91–96. [PubMed: 19118197]
20. Klopocki AG, Yago T, Mehta P, Yang J, Wu T, Leppänen A, Bovin NV, Cummings RD, Zhu C, McEver RP. Replacing a lectin domain residue in L-selectin enhances binding to P-selectin glycoprotein ligand-1 but not to 6-sulfo-sialyl Lewis x. J. Biol. Chem. 2008; 283:11493–11500. [PubMed: 18250165]
21. Lou J, Yago T, Klopocki AG, Mehta P, Chen W, Zarnitsyna VI, Bovin NV, Zhu C, McEver RP. Flow-enhanced adhesion regulated by a selectin interdomain hinge. J. Cell Biol. 2006; 174:1107–17. [PubMed: 17000883]
22. Phan UT, Waldron TT, Springer TA. Remodeling of the lectin-EGF-like domain interface in P- and L-selectin increases adhesiveness and shear resistance under hydrodynamic force. Nat. Immunol. 2006; 7:883–9. [PubMed: 16845394]
23. Lou J, Zhu C. A structure-based sliding-rebinding mechanism for catch bonds. Biophys. J. 2007; 92:1471–1485. [PubMed: 17142266]
24. Waldron TT, Springer TA. Transmission of allostery through the lectin domain in selectin-mediated cell adhesion. Proc. Natl. Acad. Sci. U. S. A. 2009; 106:85–90. [PubMed: 19118202]
25. Schindelin J, Arganda-Carreras I, Frise E, Kaynig V, Longair M, Pietzsch T, Preibisch S, Rueden C, Saalfeld S, Schmid B, Tinevez J-Y, White DJ, Hartenstein V, Eliceiri K, Tomancak P, Cardona A. Fiji: an open-source platform for biological-image analysis. Nat. Methods. 2012; 9:676–682. [PubMed: 22743772]
26. Kansas GS, Spertini O, Stoolman LM, Tedder TF. Molecular mapping of functional domains of the leukocyte receptor for endothelium, LAM-1. J. Cell Biol. 1991; 114:351–358. [PubMed: 1712791]
27. Leppänen A, White SP, Helin J, McEver RP, Cummings RD. Binding of glycosulfopeptides to P-selectin requires stereospecific contributions of individual tyrosine sulfate and sugar residues. J. Biol. Chem. 2000; 275:39569–39578. [PubMed: 10978329]

28. Nicholson MW, Barclay AN, Singer MS, Rosen SD, van der Merwe PA. Affinity and kinetic analysis of L-selectin (CD62L) binding to glycosylation-dependent cell-adhesion molecule-1. J. Biol. Chem. 1998; 273:763–770. [PubMed: 9422729]

29. Fu H, Berg EL, Tsurushita N. Fine mapping of the epitopes of humanized anti-L-selectin monoclonal antibodies HuDREG-55 and HuDREG-200. Immunol. Lett. 1997; 59:71–77. [PubMed: 9373214]

30. Leppänen A, Yago T, Otto VI, McEver RP, Cummings RD. Model glycosulfopeptides from P-selectin glycoprotein ligand-1 require tyrosine sulfation and a core 2-branched O-glycan to bind to L-selectin. J. Biol. Chem. 2003; 278:26391–26400. [PubMed: 12736247]

31. Brenner B, Gulbins E, Schlottmann K, Koppenhoefer U, Busch GL, Walzog B, Steinhausen M, Coggeshall KM, Linderkamp O, Lang F. L-selectin activates the Ras pathway via the tyrosine kinase p56lck. Proc. Natl. Acad. Sci. U. S. A. 1996; 93:15376–15381. [PubMed: 8986819]

32. Steeber DA, Engel P, Miller AS, Sheetz MP, Tedder TF. Ligation of L-selectin through conserved regions within the lectin domain activates signal transduction pathways and integrin function in human, mouse, and rat leukocytes. J. Immunol. 1997; 159:952–963. [PubMed: 9218616]

33. Li X, Steeber DA, Tang ML, Farrar MA, Perlmutter RM, Tedder TF. Regulation of L-selectin-mediated rolling through receptor dimerization. J. Exp. Med. 1998; 188:1385–1390. [PubMed: 9763619]

34. Pouyani T, Seed B. PSGL-1 recognition of P-selectin is controlled by a tyrosine sulfation consensus at the PSGL-1 amino terminus. Cell. 1995; 83:333–343. [PubMed: 7585950]

35. Zöllner O, Lenter MC, Blanks JE, Borges E, Steegmaier M, Zerwes HG, Vestweber D. L-selectin from human, but not from mouse neutrophils binds directly to E-selectin. J. Cell Biol. 1997; 136:707–716. [PubMed: 9024699]

36. Picker LJ, Warnock RA, Burns AR, Doerschuk CM, Berg EL, Butcher EC. The neutrophil selectin LECAM-1 presents carbohydrate ligands to the vascular selectins ELAM-1 and GMP-140. Cell. 1991; 66:921–933. [PubMed: 1716182]

37. Luo B-H, Strokovich K, Walz T, Springer TA, Takagi J. Allosteric beta1 integrin antibodies that stabilize the low affinity state by preventing the swing-out of the hybrid domain. J. Biol. Chem. 2004; 279:27466–27471. [PubMed: 15123676]

38. Lu C, Shimaoka M, Salas A, Springer TA. The Binding Sites for Competitive Antagonistic, Allosteric Antagonistic, and Agonistic Antibodies to the I Domain of Integrin LFA-1. J. Immunol. 2004; 173:3972–3978. [PubMed: 15356146]

39. Chen X, Xie C, Nishida N, Li Z, Walz T, Springer TA. Requirement of open headpiece conformation for activation of leukocyte integrin αXβ2. Proc. Natl. Acad. Sci. 2010; 107:14727–14732. [PubMed: 20679211]

40. Kishimoto TK, Jutila MA, Butcher EC. Identification of a human peripheral lymph node homing receptor: a rapidly down-regulated adhesion molecule. Proc. Natl. Acad. Sci. U. S. A. 1990; 87:2244–2248. [PubMed: 2179952]

41. Byron A, Humphries JD, Askari JA, Craig SE, Mould AP, Humphries MJ. Anti-integrin monoclonal antibodies. J. Cell Sci. 2009; 122:4009–4011. [PubMed: 19910492]

42. Humphries MJ, Symonds EJH, Mould AP. Mapping functional residues onto integrin crystal structures. Curr. Opin. Struct. Biol. 2003; 13:236–243. [PubMed: 12727518]

43. Sperandio M, Smith ML, Forlow SB, Olson TS, Xia L, McEver RP, Ley K. P-selectin glycoprotein ligand-1 mediates L-selectin-dependent leukocyte rolling in venules. J. Exp. Med. 2003; 197:1355–1363. [PubMed: 12756271]

44. Tsurushita N, Fu H, Melrose J, Berg EL. Epitope mapping of mouse monoclonal antibody EP-5C7 which neutralizes both human E- and P-selectin. Biochem. Biophys. Res. Commun. 1998; 242:197–201. [PubMed: 9439635]

45. Goda K, Tanaka T, Monden M, Miyasaka M. Characterization of an apparently conserved epitope in E- and P-selectin identified by dual-specific monoclonal antibodies. Eur. J. Immunol. 1999; 29:1551–1560. [PubMed: 10359109]

46. Hirose M, Kawashima H, Miyasaka M. A functional epitope on P-selectin that supports binding of P-selectin to P-selectin glycoprotein ligand-1 but not to sialyl Lewis X oligosaccharides. Int. Immunol. 1998; 10:639–649. [PubMed: 9645612]

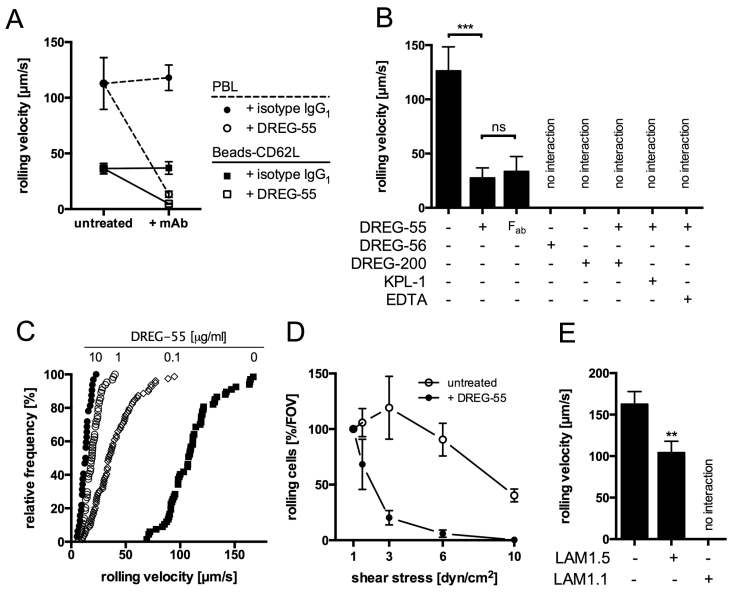

Figure 1.

Anti-human L-selectin antibodies of the DREG and LAM family differentially regulate L-selectin dependent rolling on PSGL-1.

A) The rolling velocity of human PBL (dashed line) and L-selectin (CD62L)-coated beads (solid line) was investigated in a parallel plate flow chamber on immobilized PSGL-1-F_c. PBL rolled on 30 μg/ml PSGL-1 at 2 dyn/cm^2 and beads on 20 μg/ml PSGL-1 at 3 dyn/cm^2. Anti-L-selectin mAb DREG-55 or isotype anti-human IgG_1 (10 μg/ml) were added prior to the experiment. Mean velocities were 112.8 vs. 13.3 μm/s for PBL and 36.4 vs. 4.8 μm/s for beads (untreated vs. DREG-55 mAb). Mean ± S.D is shown of n = 3-4. B) Jurkat T cells rolling on PSGL-1-F_c at 2 dyn/cm^2. 'No interaction' indicates full inhibitory activity with cell displacement equal to the hydrodynamic flow. Mean ± S.D. of 4 experiments. C) Cumulative frequency histogram of the rolling velocity showing concentration-dependent effects of DREG-55 mAb. Mean velocities are 13.1, 19.5, 39.5 and 111.5 μm/s at 10, 1, 0.1 and 0 μg/ml DREG-55 mAb concentration, respectively. 32 – 79 analyzed cells per condition, representative of 2 independent experiments. D) Jurkat cells rolling on 30 μg/ml PSGL-1 were subjected to increasing shear forces in a flow chamber. Cells were either left untreated (open circle) or incubated with 10 μg/ml DREG-55 mAb (solid circle) prior to the experiment. The number of interacting cells was determined for each shear level at 1, 1.5, 3, 6 and 10 dyn/cm^2 and expressed relatively to 1 dyn/cm^2. Mean ± S.D. of 3 experiments. FOV = field of view. E) Rolling velocity of Jurkat cells on 20 μg/ml immobilized PSGL-1 at 2 dyn/cm^2 with or without addition of LAM1.1 or LAM1.5. Mean ± S.D. of 3-4 experiments, more than 100 cells analyzed per condition.

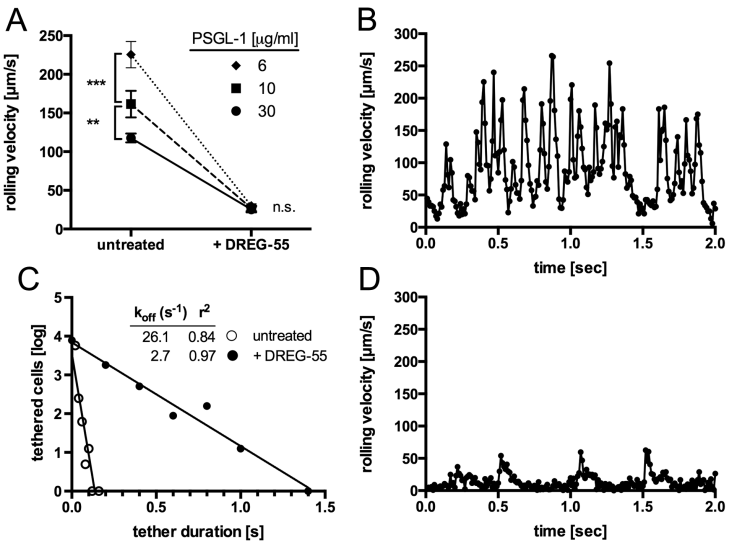

Figure 2.

Microkinetic analysis of DREG-55 mAb induced slow rolling.

A) The impact of the PSGL-1 ligand density on Jurkat cell rolling was determined with and without a saturating amount of DREG-55 mAb. Mean rolling velocities are 117.7 ± 5.8 (30 μg/ml coated ligand), 161.5 ± 17.2 (10 μg/ml) and 225.6 ± 16.8 μm/s (6 μg/ml) and decrease to 25.3 ± 3.7 (30 μg/ml), 26.7 ± 3.7 (10 μg/ml) and 29.9 ± 2.7 μm/s (6 μg/ml) upon 10 μg/ml DREG-55 treatment. Data show mean ± S.D. of n = 3 with at least 30 cells analyzed per experiment. B) and D) High-resolution velocity profile of Jurkat cells rolling on low density PSGL-1 recorded at 100 fps. A representative two second time course of an individual untreated (B) and DREG-55 antibody treated (D) Jurkat cell rolling at 0.96 dyn/cm^2 on 6 μg/ml immobilized PSGL-1 is shown. C) Comparative k_{off} values were calculated from B and D as described in methods.

Europe PMC Funders Author Manuscripts

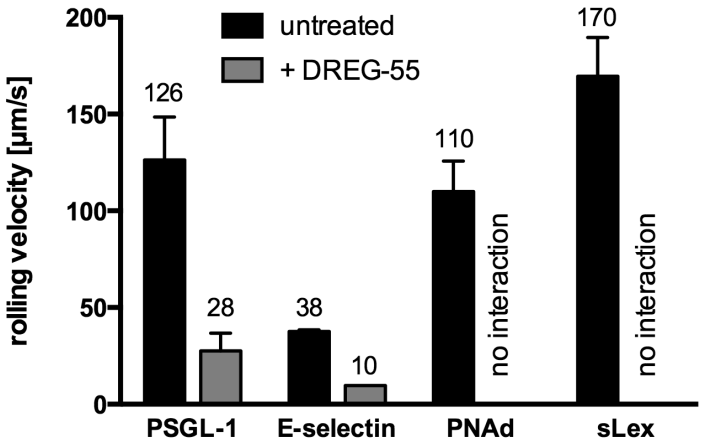

Figure 3.

DREG-55 mAb-induced slow rolling is ligand specific.

Flow chamber assays were performed with Jurkat cells at 2 dyn/cm^2 using different immobilized L-selectin ligands. Numbers on top of the bars indicate the mean rolling velocity. 'No interaction' indicates full inhibitory activity of DREG-55 mAb. DREG-200 antibody blocked all interactions (not shown). n= 3-4, mean ± S.D.

Europe PMC Funders Author Manuscripts

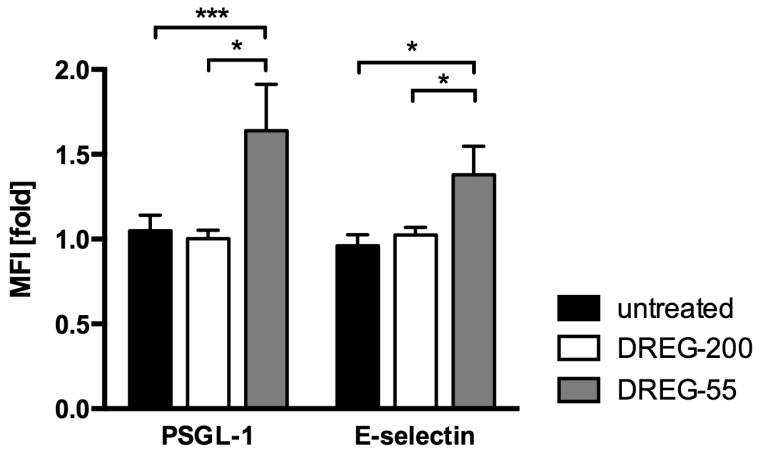

Figure 4.

DREG-55 mAb increases force-free affinity of L-selectin.

Jurkat cells were incubated with human PSGL-1-F_c or E-selectin-F_c in the presence of DREG-55 or -200 mAb and the fluorescence of the secondary anti-human IgG-FITC antibody was measured by flow cytometry. In untreated samples, only soluable ligand and secondary antibody but no DREG antibody was added. MFI is expressed relative to DREG-200 mAb samples. Mean ± S.D. of 3 to 4 experiments.

Europe PMC Funders Author Manuscripts

Europe PMC Funders Author Manuscripts

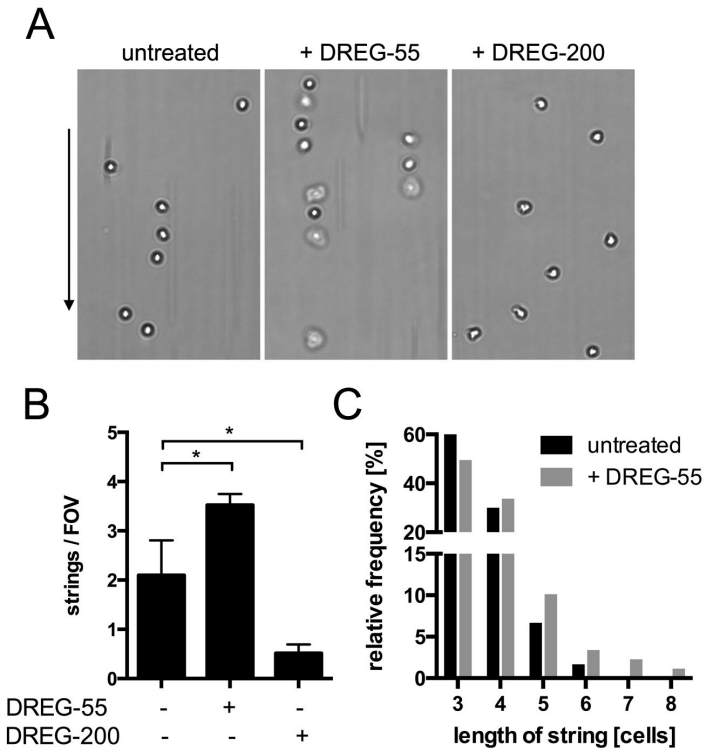

Figure 5.

PMN string formation via L-selectin-PSGL-1 interactions is enhanced by DREG-55 mAb. Flow chambers were coated with 20 μg/ml E-selectin and human PMN string formation was analyzed at 1 dyn/cm^2 as described in materials and methods. A) Typical readouts for untreated, DREG-55 and -200 mAb-treated PMNs under flow are shown. The arrow indicates the direction of the flow. B) Determination of the number of strings. 5 FOVs were averaged per experiment. Mean, n = 3 – 4. C) Histogram showing the average lengths of all strings in the untreated (n = 60) and DREG-55 treated (n = 89) condition.

Europe PMC Funders Author Manuscripts

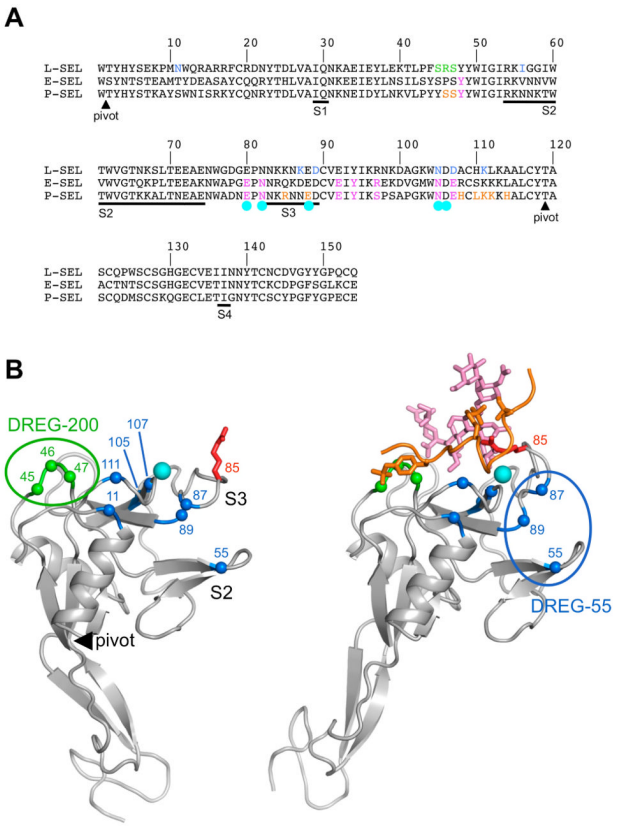

Figure 6.

Mapping of DREG antibody epitopes onto the N-terminal lectin domain.

A) Sequence alignment of the N-terminal portion of human selectins. The four switch regions in the lectin domain that undergo conformational changes upon selectin extension (19) are underlined and labeled S1-S4. Residues involved in PSGL-1 binding are indicated in orange (PSGL-1 polypeptide) and magenta (PSGL-1 glycan). Residues involved in calcium binding are marked by cyan circles. Residues whose mutation abolishes mAb DREG-55 and -200 binding (30) are indicated in blue and green, respectively. B) Cartoon drawings of P-selectin crystal structures in the bent (left panel) and extended (right panel) conformation (17). The lectin domain is at the top and the EGF-like domain at the bottom. The pivot at the interdomain hinge is indicated by a filled black triangle and switch regions S2 and S3 are labeled. The calcium ion is shown as a cyan sphere. The PSGL-1 ligand is shown in orange (polypeptide) and magenta (glycan). The two sulfated tyrosines are shown in atomic detail. Arg-85, which reorients dramatically upon PSGL-1 binding, is shown in red. Residues whose mutation abolishes DREG-55 and -200 mAb binding are indicated by blue and green Cα spheres, respectively. The putative DREG-55 mAb epitope in the extended conformation is indicated by a blue oval.

Table I

Compilation of published and our own data on anti-human selectin monoclonal antibodies binding the N-terminal lectin domain and their relation of target epitopes to relevant conformational switch regions as defined by (19) (Figure 6A). Known binding sites and differential ligand interactions are indicated as previously published. I = inhibitory, S = stimulatory, NF = non-functional, nd = not determined

				Action				
mAb-clone	**Selectin**	**Epitope residues**	**Switch**	**I**	**S**	**NF**	**Ligand**	**Sources**
EP-5C7, 1.2B6, BBIG-E6	E/P	21, 22, 23, 119, 120		X			sLe^x	(44, 45)
C215	P	76 - 83	S3			X	sLe^x	(46)
				X			PSGL-1	
TQ-1	L/E	nd		X			PPME	(16)
						X	HEV	
LAM1-1	L	nd			X		PPME	(16, 26), this report
				X			HEV, PSGL-1	
LAM1-7, 8, 9, 10, 11, 12, 13	L	nd				X	PPME	(16, 26)
						X	HEV	
LAM1-5	L	nd			X		PPME, PSGL-1	(16), this report
						X	HEV	
LAM1-6	L	nd				X	PPME	(16, 26)
				X			HEV	
LAM1-108, 110, 115, 116, 120	L	nd		X			HEV	(33)
					X		Intercellular	
DREG-55	L	11, 56, 87, 89, 105, 107, 111	S1, 3		X		PSGL-1, E-selectin	(30, 41), this report
				X			HEV, PNAd, sLe^x	
					(X)		PPME	
DREG-56	L	nd		X			PPME, HEV, PSGL-1	(41), this report
DREG-200	L	45, 46, 47		X			PSGL-1, E-selectin PNAd, sLe^x	(30, 41), this report
						X	PPME	
				(X)			HEV	